PHYSICS FROM MAMI AND ELSA TO ELFE

N. d'Hose

DAPNIA-SPhN, CE Saclay, F-91191 Gif-sur-Yvette Cedex, France
VCS and GDH collaborations, Mainz and Bonn universities, F.R.G

Abstract

This lecture relates some typical experiments with electron scattering or photon absorption in the energy range 1 - 3.5 GeV available at MAMI and ELSA in order to investigate the Nucleon structure : Nucleon electromagnetic and electro-weak form factor in elastic scattering, Nucleon polarizabilities in real and virtual Compton scattering, resonance studies in meson production, the helicity structure of the Nucleon and its resonances in the Gerasimov-Drell-Hearn sum rule experimental verification. The extension of these experiments will be streched out for higher energy 15 - 30 GeV available at ELFE.

The very fundamental experiments of Friedmann, Kendall and Taylor at SLAC in 1968 in the Deep Inelastic Scattering (DIS) regime, where short distances inside the nucleon are investigated, have given a clear evidence on the existence of point-like and nearly free charged quarks inside the nucleon. This physics at short distances is very well described by the perturbative Quantum Chromodynamics (pQCD) where the color interactions are weak. It is characterized by asymptotic freedom and the scaling laws. At large distances, color interactions are strong and confine quarks and gluons into the nucleon. This is the complex domain of the non-perturbative Quantum Chromodynamics (npQCD). The goal of the ELFE project will be to study the transition from weakly interacting quarks at small distances to the confined quarks building up the hadrons. One first way is to get precise information on specific and simple configurations of quarks in the nucleon wave function. Besides the inclusive reactions largely studied in the DIS regime, only the exclusive and hard reactions will provide some good tools for this ELFE purpose (see the lecture of Bernard Pire at this ELFE school [1]).

The measurements of exclusive reactions where particles emitted in a specific channel are observed in coincidence with the scattered electron, require a high duty cycle beam and high luminosities in order to compensate the small investigated cross section. Moreover, experiments with polarized beams are needed to disentangle specific channels through spin asymmetry measurements. Existing high energy electron accelerators have too small duty cycle ; muon and neutrino beams have too low intensity. But the new generation of low energy electron machines with large duty cycle, high currents and high polarization levels can provide opportunities for the study of exclusive measurements up to a limited Q^2.

MAMI comprises a linac injector followed by 3 microtrons in cascade in order to provide an electron beam of 855 MeV energy with a resolution of 10^{-4}, 100% duty cycle, and high intensity up to 100 μA . Polarized electrons are produced by laser induced photoemission on a GaAsP crystal. A polarization of 32% is reached at 10 μA, and 75% at 2 μA. The technics of spin polarized $^3\vec{\mathrm{He}}$ gas target is well over-controlled .

ELSA is a synchrotron accelerator of 2.5 GeV followed by a stretcher ring in order to improve the duty factor and to increase the available energy up to 3.5 GeV. Important technics on frozen spin polarized targets are developed.

A typical exclusive reaction on a nucleon in electron scattering is $eN \to e'N'X$. The nucleon (proton or neutron of mass m) is still present in the final state. The produced particle denoted X (if we are not in the elastic case) is a photon or a meson of mass m'. We consider only ultra-relativistic electrons ($m_e = 0$) and the case of one photon exchange. (The contribution of diagrams where a Z^0 or two or more virtual photons are exchanged is neglected at the first order of the electromagnetic coupling constant α_{QED}). We use k, k', p, p', q, q' to denote the 4-momenta of the initial and final electrons, initial and final nucleons, virtual photon, and produced particle respectively. The important kinematical variables are :

- The 4-momentum of the virtual photon : $q^\mu = k^\mu - k'^\mu$ which depends only on the electrons kinematics (electrons energies (E, E') and scattering electron angle θ in the Laboratory frame). We often use the Laboratory energy of the virtual photon $\nu = E - E'$.

- The invariant mass of the virtual photon : $q^\mu q_\mu = -Q^2 < 0$ which is always negative. One says that the virtual photon is space-like. Its expression in the Laboratory frame is $Q^2 = 4EE' \sin^2 \theta/2$.

- The invariant polarization ϵ of the virtual photon which expression in the Laboratory frame is $\epsilon = (1 + 2\frac{\nu^2+Q^2}{Q^2} \tan^2 \theta/2)^{-1}$.

- The invariant s or the center of mass energy square of the (virtual photon + nucleon) system is $s = (p+q)^2 = (p'+q')^2 \geq m^2$. This limit is the elastic scattering.

- The invariant t or the transfer to the nucleons is $t = (p - p')^2$. A hard reaction implies large $\mid t \mid$, and also large transverse momentum. The production angle in the center of mass $\theta_{qq'}$ has to be large ($\sim 90°$) : $\mid q'_T \mid = \sin \theta_{qq'} (s - m^2 + m'^2)/2\sqrt{s}$.

This lecture reports some typical reactions which are studied at MAMI or ELSA, and their outlook at the ELFE facility :

- Elastic electron-nucleon scattering, which is defined by $s = m^2$, is specified by the electric and magnetic nucleon form factors $G_E(Q^2)$ and $G_M(Q^2)$ or, equivalently, the Dirac and Pauli form factors $F_1(Q^2)$ and $F_2(Q^2)$. These form factors are directly related to the distribution of charge and magnetization currents inside the nucleon of definite size. They are the basic observables related to the structure of nucleons that one would like to understand in terms of fundamental constituents. We present the improvement in the knowledge of the small value of $G_E^n(Q^2)$ in the range $Q^2 = 0.2 - 0.6$ GeV^2, which is investigated at MAMI by the measurement of the polarization asymmetry with polarized electrons and a polarized $^3\vec{\mathrm{He}}$ gas target. This kind of experimental method will be continued at ELFE in the hard region at high Q^2.

- Parity violation in elastic scattering of polarized electrons on the nucleon is studied at MAMI to investigate the electro-weak form factor of the proton.

- The next simplest exclusive reaction is the electroproduction of photons. Virtual Compton scattering in the low s regime below the pion photoproduction threshold ($m \leq \sqrt{(s)} \leq m + m_\pi$, but arbitrary Q^2) provides new electromagnetic observables (functions of Q^2 as the form factors) which generalize the usual electric (α) and magnetic (β) polarizabilities that are measured using real photons. They are controlled by the excitation spectrum of the nucleon. Nevertheless, the excited states or resonances contribute only virtually and the "generalized" polarizabilities are very clean probes of the non-perturbative structure of the nucleon. The hard regime at large t and s will be studied at ELFE for the investigation of the proton valence wave function.

- When $\sqrt{s}$ is in the range 1.2 to 2 GeV^2 meson production linked to the decay of the nucleon resonances becomes the dominant process. Single-pion photoproduction has been extensively studied since the 1960's, and is governed by the excitation of nucleon resonances. The cross section, as a function of the photon excitation energy, presents three main peaks : the M1 magnetic dipole excitation which is essentially related to the $\Delta(1232)$ excitation, the E1 electric dipole excitation and the E2 electric quadrupole excitation which are mainly due to the $D_{13}(1520)$ and $F_{15}(1680)$ resonances respectively. Nevertheless, there is also a large number of weakly excited states with considerable overlapping due to their large resonance width. Other decay channels reveal differently the resonances. The isoscalar η meson production is strongly dominated by the $S_{11}(1535)$ resonance. The production of η has been very accurately studied at MAMI and ELSA. The reader will find reports in the different references [2]. The production of ϕ mesons will be studied at ELSA at small t and pursued at ELFE at large t.

- The Gerasimov-Drell-Hearn (GDH) sum rule relates the helicity structure of the photoproduction cross section to the anomalous magnetic moment of the nucleon. The evaluation of the sum rule depends on our knowledge of the contribution of all the resonances. To derive the sum rule we use only general principles : Lorentz and gauge invariance, crossing symmetry, causality and unitarity. A generalized GDH sum rule may be derived for virtual photons. At high Q^2 it may be expressed in terms of the parton spin distributions which are measured in deep inelastic scattering. A first experiment using circularly polarized electrons and longitudinally polarized protons is proposed at MAMI and ELSA.

- Looking to the future, these exclusive experiments will be extended to the hard regime provided by the ELFE facility.

1 Elastic scattering

1.1 Electromagnetic Nucleon Form factor

We recall the general formalism for the elastic cross section and use the kinematical notation defined in the introduction (we note $\tau = Q^2/4m^2$).

Spin 1/2 electron scattering on spin 1/2 structureless target (e.g. muon)

$$\frac{d\sigma}{d\Omega} = \frac{\alpha^2_{QED}}{4E^2 \sin^4 \theta/2} \times \cos^2 \theta/2 \times (1 + 2\tau \tan^2 \theta/2) \times \frac{E'}{E} \tag{1}$$

The origin and the meaning of the different terms can be seen as :

- the first term is the Rutherford cross section which corresponds to an electron without spin, scattering on spinless pointlike particle with an infinite mass.
- the $\cos^2 \theta/2$ term comes from the spin 1/2 of the electron. The product of the first two terms corresponds to $\frac{d\sigma}{d\Omega}_{Mott}$ with its characteristic behaviour $\frac{d\sigma}{d\Omega}_{Mott} \overset{\theta \to 0}{\to} \theta^{-4}$
- the $\frac{E'}{E}$ terms comes from the recoil of the target of finite mass.
- $(1 + 2\tau \tan^2 \theta/2)$ comes from the spin 1/2 pointlike target for its magnetic interaction with the spin 1/2 electron.

Extended structure of the nucleon of anomalous magnetic moment κ

Lorentz and gauge invariance together with parity conservation imply that the proton electromagnetic current is parametrized by 2 invariants : the Dirac ($F_1(Q^2)$) and Pauli ($F_2(Q^2)$) form factors.

$$\frac{d\sigma}{d\Omega} = \frac{d\sigma}{d\Omega}_{Mott} \frac{E'}{E} \left[(F_1^2 + \kappa^2 \tau^2 F_2^2) + 2\tau (F_1 + \kappa F_2)^2 \tan^2 \theta/2 \right] \tag{2}$$

If the nucleon was pointlike, then $F_2 = 0$ and $F_1 = 1$.
At $Q^2 = 0$, $F_1^p = 1$, $F_1^n = 0$, $F_2^p = 1$, $F_2^n = 1$.
One defines also the Sachs form factors such as :

$$G_E(Q^2) = F_1(Q^2) - \kappa\tau F_2(Q^2) \qquad \text{and} \qquad G_M(Q^2) = F_1(Q^2) + \kappa F_2(Q^2) \tag{3}$$

$$\frac{d\sigma}{d\Omega} = \frac{d\sigma}{d\Omega}_{Mott} \frac{E'}{E} \left[\frac{G_E^2 + \tau G_M^2}{1 + \tau} + 2\tau (G_M)^2 \tan^2 \theta/2 \right] \tag{4}$$

At $Q^2 = 0$, $G_E^p = 1$, $G_E^n = 0$, $G_M^p = 1 + \kappa_p = \frac{\mu_p}{\mu_N}$, $G_M^n = \kappa_n = \frac{\mu_n}{\mu_N}$, where $\mu_N = \frac{e\hbar}{2m}$ is the nuclear magneton. One finds $\mu_p = 2.79\mu_N$ (Stern 1933) and $\mu_n = -1.91\mu_N$ (Alvarez-Bloch 1939).

Physical interpretation of G_E and G_M

If we work either in the proton Breit frame or with ν small compared to the mass of the proton, then G_E is the Fourier transform of the hadron charge density :

$$G_E(\vec{q}) = \int \rho(\vec{r}) e^{i\vec{q}.\vec{r}} d\vec{r} \tag{5}$$

If $|\vec{q}|$ is small, G_E can be expressed as an expansion of $|\vec{q}|$: $G_E(\vec{q}) = 1 - \frac{q^2}{6} < r^2 >_{charge} + ...$

$$< r^2 >_{charge} = -6 \left(\frac{\partial G_E(\vec{q}}{\partial q^2} \right)_{Q^2=0} \tag{6}$$

$< r_p^2 >_{charge} = 0.862 \pm 0.012$ fm^2 and $< r_n^2 >_{charge} = -0.116 \pm 0.002$ fm^2.
In the same way G_M is related to the hadron magnetization density.

Experimental measurement : Rosenbluth separation and limit

In the elastic case $Q^2 = 2m\nu$ and $\epsilon = (1 + 2(1+\tau)\tan^2\theta/2)^{-1}$, so we can write :

$$\frac{d\sigma}{d\Omega} = \frac{d\sigma}{d\Omega}_{Mott}\frac{E'}{E}\frac{1}{\epsilon(1+\tau)}\left[\epsilon G_E^2 + \tau G_M^2\right] \tag{7}$$

This expression shows that by measuring cross sections at the same value of Q^2, q, ν but for different values of θ, E, E', we can separate the 2 form factors : this is the principle of the Rosenbluth separation. This technique has provided us with an important set of data on the electromagnetic form factors of the proton which has been recently extended up to 9 GeV^2[3]. This appears to be the limit of the Rosenbluth technique : for higher Q^2 the electric contribution to the cross section is smaller, and also smaller relative to the magnetic one, so that its extraction becomes very difficult. Nevertheless, in the limit $\epsilon G_E^2 \ll G_M^2$ the cross section depends only on G_M which can be extracted from the data. This was done to 32 GeV^2[4]. In order to measure G_E at higher Q^2, we have to use polarization techniques, which allows its determination through an interference term between G_E and G_M.

Proton form factor

At the first order, the proton form factors are described by the dipolar approximation, which was introduced by Hofstadter in the 1950's, viz.

$$\frac{G_E^p(Q^2)}{G_E^p(0)} = \frac{G_M^p(Q^2)}{G_M^p(0)} \simeq (1 + \frac{Q^2}{0.71\mathrm{GeV}^2})^{-2} \tag{8}$$

The deviations from a dipole form at low momentum transfer is of the order of 5% for G_M and reaches 20% for G_E which is more poorly measured. Several models attempt to reproduce the exact behaviour of the form factors. They are based on vector dominance models, or QCD sum rules, or diquark model, or relativistic constituent quark model, or hybrid models which try to reconcile a mesonic models at low Q^2 and pQCD at high Q^2. None of these models characterize fully the data over the whole Q^2 range.

At high Q^2 (above 10 GeV^2), the scaling laws predict that the magnetic form factor varies as Q^{-4} (with a small pQCD scaling violation) – see Section 4.

Neutron form factor

Compared to the proton, little progress has been made on the neutron charge and magnetic form factors. In particular, the information on G_E^n is still rather limited and is based on two experimental methods :

- thermal neutron scattering from atomic electrons gives a mean squared charge radius $< r_n^2 >_{charge}$ which provides a value of the slope $\left(\frac{\partial G_E(\vec{q})}{\partial q^2}\right)_{Q^2=0} \simeq 0.019$ fm^2.
- at small Q^2 (≤ 1 GeV^2) the elastic electron-deuteron scattering gives access to G_E^n with good statistics but with a large systematic error (a factor 2) since this method depends on the nucleon-nucleon potential used to extract the neutron information from the deuteron.

An improved experimental method is now available in polarized electron-neutron $(\vec{e}, \vec{n})$ scattering. In constrast to the unpolarized cross section measurement, for which the effect of the electric scattering cross section is submerged by the much larger magnetic one, the polarization asymmetry has a component which is proportional to an interference term between the electric and magnetic scattering amplitudes. The high duty cycle and the high current polarized beam of the accelerator MAMI offer the possibility for the exclusive reaction $^3\vec{\mathrm{He}}(\vec{e}, e'n)$ (where $^3\vec{\mathrm{He}}$ contains an approximately saturated spin pair of two protons and therefore only the contribution of the neutron dominates). This experiment was presented in detail at this ELFE School by John Annand [5]. The first measurement at $Q^2 = 0.31$ GeV^2 of G_E^n to $\pm 10\%$ accuracy demonstrates the powerful new method of using spin observables, and will encourage measurements in the accessible momentum transfer range of MAMI : $0.2 \leq Q^2 \leq 0.6$ GeV^2.

1.2 Electroweak form factor

Consider elastic scattering with polarized electrons, viz. $\vec{e}p \to ep$. The electromagnetic interaction which is determined by the exchanged of one virtual photon (at the first order) respects parity conservation. However, this is not the case for the weak interaction characterized by the exchange of a neutral vector boson Z^0; the asymetry $A = \frac{\sigma_{1/2} - \sigma_{-1/2}}{\sigma_{1/2} + \sigma_{-1/2}}$ is parity violating. The leading parity violating term is given by an interference term between the exchange of a photon and a Z^0, and therefore between electromagnetic F^γ and electroweak F^Z form factors of the proton, thus enabling us to extract this electroweak form factor.

In the Standard Model, the couplings of the Z^0 to the quarks are known. If we consider the SU(3) symmetry, it is possible to express the electromagnetic and electroweak form factors of proton and neutron in terms of the quantities F^u, F^d, F^s (corresponding to scattering from up, down and strange quark components of the nucleon's wavefunction respectively):

$$
\begin{aligned}
F^{\gamma p} &= 2/3F^u - 1/3F^d - 1/3F^s && (9)\\
F^{\gamma n} &= 2/3F^d - 1/3F^n - 1/3F^s && (10)\\
F^{Zp} &= (1/2 - sin^2\theta_W)F^{\gamma p} - 1/12(F^u + F^d + F^s) && (11)
\end{aligned}
$$

The proton electroweak form factor measurement gives us three independent linear combinations of F^u, F^d, F^s, whence we can extract F^s (the strange quark contribution in the nucleon).

The asymmetry is very small ($10^{-4}Q^2$). Several experiments at MAMI, CEBAF and Bates are devoted to this goal. At MAMI, the experiment is planned to measure an asymmetry with an accuracy of 3%, thank to the very high luminosity $\mathcal{L} \sim 10^{38} cm^{-2}s^{-1}$ and a large acceptance calorimeter[6].

2 Real and virtual Compton scattering

2.1 Polarizabilities

Virtual Compton Scattering in the low s regime below the pion photoproduction threshold ($m \leq \sqrt{(s)} \leq m + m_\pi$, but arbitrary Q^2) gives us the opportunity to measure the nucleon polarizabilities. They are fundamental electromagnetic observables of the nucleon, functions of Q^2, and are complementary to the elastic form factors. At $Q^2 = 0$ with real photons, we get the usual electric (α) and magnetic (β) polarizabilities. In the energy domain provided at MAMI and then CEBAF, we can measure these observables in the range $Q^2 = 0.15 - 0.40$ GeV^2 and $Q^2 = 1. - 3.$ GeV^2 respectively.

The idea behind the concept of electromagnetic polarizabilities can be easily understood by a comparison with classical physics. If we consider an electron (of charge $-e$ and mass m_e) moving inside a sphere of radius a and total charge $+e$ uniformly distributed (atomic Thomson model), the local electric field acting on the electron is :

$$\vec{E}_{local} = \frac{e}{4\pi\epsilon_0}\frac{\vec{r}}{a^3} = \frac{m_e\omega_o^2}{e}\vec{r} \tag{12}$$

The electron is constrained by a spring strength (of constant ω_0). If an external electric field $\vec{E_{ext}} = \vec{E}_o e^{-i\omega t}$ polarizes the system, an electric dipole moment $\vec{d}$ is induced :

$$\vec{d} = -e\vec{r} \equiv \alpha\vec{E}_{ext}, \tag{13}$$

where α is defined as the polarizability. The dynamical equation applied to the electron gives :

$$\alpha = \frac{e^2}{m_e}\frac{1}{(\omega_0^2 - \omega^2)} \quad \overset{\omega\to 0}{\to} \quad 4\pi\epsilon_0 a^3 \tag{14}$$

The denominator of the general formula indicates clearly that the polarizability determines the stiffness of the system which is related to its internal structure. We note easily that the dimension of the polarizability in this case is a volume.

The radiative power of this system, denoted $P_{Rayleigh}$, is given by the antenna formula and can be related to the electromagnetic energy density u_{em} and the Rayleigh cross section :

$$P_{Rayleigh} = \frac{<\ddot{\vec{d}}>^2}{6\pi\epsilon_0 c^3} = u_{em}c \times \sigma_{Rayleigh} \tag{15}$$

$$\sigma_{Rayleigh} = \frac{\alpha^2}{6\pi\epsilon_0^2 c^4}\omega^4 = \sigma_{Thomson}\frac{\omega^4}{(\omega_o^2 - \omega^2)^2} \tag{16}$$

Here $\sigma_{Thomson} = \frac{8\pi}{3}r_0^2$ is obtained for the free electrons ($\omega_0 = 0$) and $r_0 = \alpha_{QED}/m_e$ is the classical radius of the electron.[1] The Rayleigh scattering is proportional to α^2 and ω^4, which implies the well-known phenomena of blue skies and red sunsets.

Let we derive the quantum mechanical expression of the polarizability. The eigenstates of a system are noted $|0>, ...|N>$ with eigen energies $E_0, ...E_N$. If we apply a perturbation W with an external electric field parallel to the z direction, $W = -\vec{d}.\vec{E}_{ext} = -d_z E_{ext}$. The new eigenstates can be evaluated at the first order of the perturbation with :

$$|0'> = |0> - \sum_{N\neq 0}\frac{<N|W|0>}{E_N - E_0}|N> + O(W^2) \tag{17}$$

[1] In this classical calculation, we use the MKSA unity system where $\alpha_{QED} = e^2/4\pi\epsilon_0\hbar c$. In the Real Compton Scattering, the theory of which has been known for several decades, we use the Gauss unity system : $\alpha_{QED} = e^2$. In the Virtual Compton Scattering, more recently developed in terms of "generalized" polarizabilities, we use the Heaviside unity system : $\alpha_{QED} = e^2/4\pi$.

An electric dipole moment $\vec{d}$ is induced : $<\vec{d}>= \alpha \vec{E_{ext}}$

$$<d_z>=<0'|d_z|0'>=<0|d_z|0> +2E_{ext}\sum_{N\neq 0}\frac{|<N|d_z|0>|^2}{E_N-E_0}+... \tag{18}$$

For a symmetrical system, the first term is zero, so the polarizability has the general formula :

$$\alpha = 2\sum_{N\neq 0}\frac{|<N|d_z|0>|^2}{E_N-E_0} \tag{19}$$

This formula has the same form as the previous expression obtained using classical mechanics if we multiply both the numerator and denominator by r^2. It has the advantage that it shows clearly that we are sensitive to the whole excitation spectrum of the system. Because of the threshold condition, the excited states contribute virtually. This is an advantage over real resonance production for which meson production and rescattering are the dominant process and must be treated explicitly even though they are not the interesting part of the problem in so far as nucleon structure is concerned. Below the pion production threshold, the situation is simpler because the excited states cannot decay and therefore have no width, which is the hypothesis of most theoretical models of nucleon structure. This advantage is similar to the Deep Inelastic Scattering regime for which it makes sense to use the parton model because the partons fragmentation can be neglected [7].

2.2 Real Compton Scattering

Let us consider Compton scattering on a nucleon of charge e and mass m. Let $\vec{q}$ and $\vec{\epsilon}$ be the momentum and polarization vectors of the incoming photon, $\vec{q'}$ and $\vec{\epsilon'}$ the corresponding ones for the scattered photon at an angle θ in the Laboratory frame. We have the usual Compton formula $\nu' = \nu/(1+\frac{\nu}{m}(1-cos\theta))$. The photon energies are $\nu = |\vec{q}|$ and $\nu' = |\vec{q'}|$ respectively. The amplitude for low-energy Compton scattering (without polarization measurement) when expanded to second order in ν is [8],[9] :

$$T(\gamma N \to \gamma N) = -\left(\frac{e^2}{m} - \frac{e^2<r^2>}{6m}(\vec{q}^2+\vec{q'}^2)+\alpha\nu\nu'\right)\vec{\epsilon}\vec{\epsilon'} + \beta(\vec{\epsilon}\wedge\vec{q})(\vec{\epsilon'}\wedge\vec{q'}) + 0(\nu^3) \tag{20}$$

We recognize first the constant Thomson term and then a modified Rayleigh term. The differential cross section as a function of the scattering angle is :

$$\frac{d\sigma}{d\nu} = \frac{d\sigma_{point}}{d\nu} - \frac{e^2}{m}\left[\frac{\nu'}{\nu}\right]^2 \nu\nu'\left[\frac{\bar{\alpha}+\bar{\beta}}{2}(1+cos\theta)^2 + \frac{\bar{\alpha}-\bar{\beta}}{2}(1-cos\theta)^2\right] + 0(\nu^4) \tag{21}$$

where $d\sigma_{point}/d\nu$ is the Powell cross section, the one for the Compton Scattering on a pointlike nucleon (with charge, spin and also anomalous magnetic moment). The Compton scattering polarizabilities $\bar{\alpha}$ and $\bar{\beta}$ are not equal to the static ones [8],[9].

$$\bar{\alpha} = 2e^2\sum_{N\neq 0}\frac{|<N|d_z|0>|^2}{E_N-E_0} + \frac{e^2<r^2>}{3m} \tag{22}$$

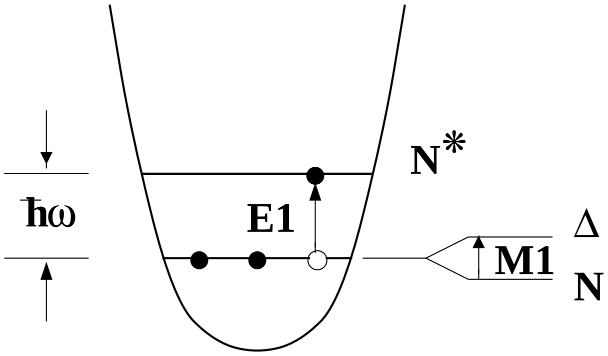

Figure 1: *Electric and magnetic dipole interactions in a naive oscillator quark model.*

$$\bar{\beta} = 2e^2 \sum_{N \neq 0} \frac{|< N|\mu_z|0 >|^2}{E_N - E_0} - \frac{e^2 < r^2 >}{6m} - \frac{e^2 < d^2 >}{2m} \tag{23}$$

$\bar{\alpha}$ and α differ by a positive correction factor which is due to the retardation effect. For the magnetic polarizability the corrections are more subtle. We have two negative (diamagnetic) contributions : one is due to a counterpart in the retardation effect, the other is due to finite size effects in the seagull term.

It can be read from the expression for the cross section, eq.(21), that in the forward direction one measures $\bar{\alpha}+\bar{\beta}$, in backward direction one measures $\bar{\alpha}-\bar{\beta}$ and that at 90° $\bar{\alpha}$ is determined alone. A sum-rule for $\bar{\alpha}+\bar{\beta}$ is described in equ.(63) – see Section 3. One finds $\bar{\alpha}+\bar{\beta} = (14.2 \pm 0.3)10^{-4}$ fm^3. Several experiments whose references are in [10] were devoted to these measurements and provide mean values $\bar{\alpha} = (11.8 \pm 0.9)10^{-4}$ fm^3 and $\bar{\beta} = (2.5 \pm 0.9)10^{-4}$ fm^3. Now a new experiment [10] is forseen at MAMI in order to give a significant improvement in the precision on $\bar{\alpha}$ and $\bar{\beta}$.

There is a simple interpretation of the value of the polarizabities [8]. For α, the electric dipole moment operator implies only the N^* excited states which can be reached by an E1 transition. A set of such resonances with spin and parity $J^\pi = 1/2^-, 3/2^-$ exists in a range of excitation energies $\simeq 650$ MeV. If we use the empirical proton charge radius, we find $\alpha_p \sim \frac{2}{3}\frac{e^2 <r_p^2>}{\Delta E} \sim 10^{-3}$ fm^3 which is roughly the correct order of magnitude. For β, the magnetic response is dominated by the strong M1 transition from the nucleon to the $\Delta(1232)$. This gives a large paramagnetic contribution of 10^{-3} fm^3, which has to be balanced by a substantial diamagnetic part.

The Non-Relativistic Constituent Quark Model which was developed by Isgur and Karl[11] has essentially three parameters. The basic degrees of freedom are massive constituent quarks (of mass $m \simeq 0.34$ GeV) moving within a harmonic oscillator confining potential (with a parameter $\bar{h}\omega \simeq 500$ MeV) and additional hyperfine interactions (with a chromomagnetic fine structure constant). The oscillator parameter of the confining potential can be estimated from the masses of the lowest negative parity (p-shell) N^* resonances as compared to the average mass of the nucleon and the $\Delta(1232)$ (these latter are both on the s-shell, they only differ by a spin-flip of one quark). The electric and magnetic polarizabilities are governed by the $N \to N^*$

and $N \to \Delta$ transitions respectively, as illustrated in Fig. 1. In this model, the value of the magnetic polarizability is quite good, but the electric polarizability is really too small (about half the experimental value).

One of the limitations of the Non-Relativistic Constituent Quark Model is that it has no relationship to chiral symmetry, an important property of QCD which governs much of low energy hadron physics. Chiral symmetry is spontanously broken ; the pion is the corresponding Goldstone boson. All the models which unify quark and meson degrees of freedom such as Cloudy Bag and Chiral Bag give better results for the two polarizabilities. This implies that the electric polarizability is clearly related to the pion cloud.

It is then really important to increase the number of measured observables and to see their evolution in different domain of Q^2 in order to compare the different theoretical models of the nucleon. This is the goal of the Virtual Compton Scattering which will provide the "generalized" polarizabilities.

2.3 Virtual Compton Scattering

This exclusive reaction $ep \to e'p'\gamma'$ is defined by five kinematical independant variables : ϵ, Q^2, s, (these three ones depend only on the electron kinematics), $\theta_{\gamma\gamma}$ (noted also for convenience θ) (angle between the two photons) and ϕ (azimuthal angle of the electron plane with respect to the hadron plane). Since we are in a kinematical regime defined by a center of mass (CM) energy ($\sqrt{s}$) of the final proton-photon system close to threshold and below pion photoproduction threshold, it is natural to work in the CM frame and to use q and q' the modulus of the momentum of the real and virtual photon respectively, instead of Q^2 and s. The relations between these two sets of variables are $q' = (s - m^2)/2\sqrt{s}$ and $q = (Q^2 + (s - Q^2 - m^2)^2/4s)^{\frac{1}{2}}$; q' varies from 0 to $\sim$125 MeV.

The cross section has the form :

$$\frac{d^5\sigma}{d\mathrm{k'}_{lab}[d\Omega_e]_{lab}[d\Omega_p]_{CM}} = \frac{(2\pi)^{-5}}{64m} \left(\frac{\mathrm{k'}_{lab}}{\mathrm{k}_{lab}}\right) \frac{s - m^2}{s} \times \mathcal{M}^{exp} \tag{24}$$

where $\mathcal{M}^{exp}$ is invariant under a Lorentz transformation.

In this reaction, the final photon can be emitted either by the electron or by the proton. The first process is described by Bethe-Heitler (BH) amplitude which is calculable from Quantum Electro-Dynamics (QED). The second process is described by the Full Virtual Compton Scattering ($FVCS$) amplitude which, in the one photon exchange approximation, is a linear combination of VCS amplitudes. Assuming that the one photon exchange approximation is valid, the BH and $FVCS$ amplitudes correspond to the graphs shown in Fig 2.

The probability $\mathcal{M}^{exp}$ is a coherent sum of two matrix elements,

$$\mathcal{M}^{exp} = \frac{1}{4} \sum_{\sigma\sigma' h' \lambda'} |T^{ee'\gamma}|^2 = \frac{1}{4} \sum_{\sigma\sigma' h' \lambda'} |T^{BH} + T^{FVCS}|^2 \tag{25}$$

where T^{BH} and T^{FVCS} are respectively the matrix elements for the Bethe Heitler (BH) and Full Virtual Compton Scattering (FVCS) processes. In the one photon exchange approximation,

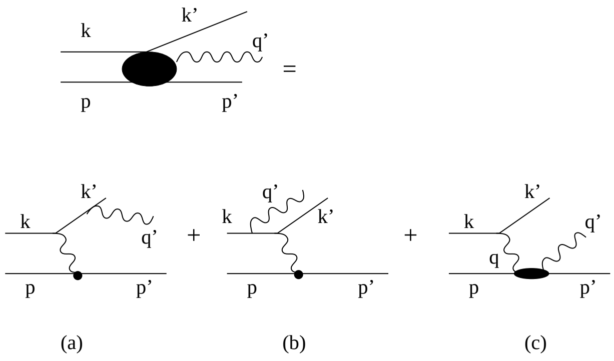

Figure 2: *The $p(e,e'p)\gamma$ reaction. The initial, final electron and initial, final proton quadri-momenta are k, k' and p, p' respectively. The final photon quadri-momentum is q'. a) and b) correspond to the Bethe-Heiler (BH) process. c) corresponds to the Full Virtual Compton Scattering (FVCS) process. We note q the quadri-momentum of the virtual photon exchanged in the FVCS process, that is $q = k - k'$.*

one has :

$$T^{FVCS} = \frac{-e^3}{Q^2} \sum_\lambda \Omega(h,\lambda) T^{VCS}(\lambda',\lambda) \tag{26}$$

where λ is the virtual photon helicity, T^{VCS} is the Virtual Compton Scattering off the proton and $\Omega(h,\lambda)$ the lepton current ($e^2 = 4\pi/137$ in Heaviside units). One writes :

$$T^{VCS} = T^N + R \tag{27}$$

where T^N is the nucleon contribution and R is the contribution of the higher energy states. The latter start at $\sqrt{s} = m + m_\pi$ which guaranties that the energy denominators do not vanish at the soft photon point. So the sum R over all the possible excited states is regular.
Nevertheless, following Ref.[7], the most transparent analysis of Virtual Compton Scattering is to split the VCS amplitude into two terms:

- the Born term which contains only the on-shell nucleon and anti-nucleon contributions. This term is gauge invariant in the Dirac and Pauli form factor decomposition. It is exactly calculable once we know these form factors at the Q^2 of interest.
- the Non-Born term which is $T^{NonBorn} = T^{VCS} - T^{Born}$

In an expansion in powers of **q'**, the first terms of the amplitudes T^{BH} and T^{Born} are of order q'^{-1}, whilst the first term of $T^{NonBorn}$ is of order q' according to Low's theorem [12]. It follows that:

$$T^{ee'\gamma} = \underbrace{T^{BH} + \frac{-e^3}{Q^2}\sum \Omega . T^{Born}}_{\alpha_{-1}\mathrm{q}'^{-1} + \alpha_0 \mathrm{q}'^0 + \alpha_1 \mathrm{q}' + 0(\mathrm{q}'^2)} + \underbrace{\frac{-e^3}{Q^2}\sum \Omega . T^{NonBorn}}_{\beta_1 \mathrm{q}' + 0(\mathrm{q}'^2)} \tag{28}$$

where $\alpha_{-1}, \alpha_0, \alpha_1$ are known functions of the kinematical variables $(\mathrm{q}, \epsilon, \theta, \varphi)$. T^{BH} and T^{Born} are completely calculable once the elastic form factors of the proton are known.

The term β_1 is related to the first derivative of the Non-Born term with respect to q′ evaluated at $\mathrm{q}' = 0$. It is proton structure dependent and can be parametrized by 10 real functions of Q^2 or q. (At $\mathrm{q}' = 0$, we have $Q^2 = -2m^2 + 2m\sqrt{m^2 + \mathrm{q}^2}$). The coefficients of the parametrisation contain the dependence in the variables $(\mathrm{q}, \epsilon, \theta, \varphi)$. The 10 functions are distinguished by the spin flip or non spin flip character of the reaction and by the total angular momentum of the photons. In the Non Born term, which is linear in q′, the final photon can only be dipole electric or magnetic while for finite Q^2 the initial photon is only restricted by parity and angular momentum conservation. The selection rules used to determine the number of these functions originate from parity and total angular momentum conservation as expressed in equations :

$$\begin{array}{ll} (-1)^{\rho+L} = (-1)^{\rho'+L'} & \rho, \rho' = 0, 1, 2 \\ |L - L'| \le S \le L + L' & S = 0, 1 \end{array} \tag{29}$$

The index ρ (resp. ρ') refers to the electric (2), magnetic (1) and longitudinal (0) character of the initial (resp. final) photon. L is the total angular momentum of the initial photon (L'=1 for the final photon) and S refers to the spin (S=1) and non spin-flip (S=0) character of the transition. Table 1 presents the possible quantum numbers of these functions $\beta_1^{(\rho' L', \rho L)S}$.

Polarizabilities					
ρ'	ρ	**L**	**S**	**Multipole** $(\gamma^{real}, \gamma^{virtual})$	**notation** $\beta_1^{(\rho' L', \rho L)S}$
1	0	0,2	1	$(M1, L0), (M1, L2)$	$\beta_1^{(11,00)1}, \beta_1^{(11,02)1}$
	2	2	1	$(M1, E2)$	$\beta_1^{(11,22)1}$
	1	1	0,1	$(M1, M1)$	$\beta_1^{(11,11)0}, \beta_1^{(11,11)1}$
2	0	1	0,1	$(E1, L1)$	$\beta_1^{(21,01)0}, \beta_1^{(21,01)1}$
	2	1	0,1	$(E1, E1)$	$\beta_1^{(21,21)0}, \beta_1^{(21,21)1}$
	1	2	1	$(E1, M2)$	$\beta_1^{(21,12)1}$

Table 1: *Conventions for the notation of the involved multipoles. The index ρ (resp. ρ') refers to the electric (2), magnetic (1) and longitudinal (0) character of the initial (resp. final) photon. L is the total angular momentum of the initial photon (L'=1 for the final photon) and S refers to the spin (S=1) and non spin-flip (S=0) character of the transition.*

To parametrize these 10 functions, one needs 10 "generalized polarizabilities" :

$$\begin{array}{ccccc} P^{(11,00)1} & P^{(11,02)1} & P^{(11,11)0} & P^{(11,11)1} & \hat{P}^{(11,2)1} \\ P^{(01,01)0} & P^{(01,01)1} & P^{(01,12)1} & \hat{P}^{(01,1)0} & \hat{P}^{(01,1)1} \end{array} \tag{30}$$

which have been defined in such a way that their limit at $\mathrm{q} \to 0$ is the same as the real photon limit. We use $\tilde{q}_0$ to denote the energy of the virtual photon at $\mathrm{q}' = 0$; $\tilde{q}_0 = m - \sqrt{m^2 + \mathrm{q}^2} \overset{\mathrm{q} \to 0}{\to}$

$\frac{q^2}{2m}$. The parametrization is :

$$
\begin{aligned}
\beta_1^{(11,\rho L)S}(\mathrm{q}) &= \mathrm{q}^L\, P^{(11,\rho L)S}(\mathrm{q}) \qquad (\rho=0,1) \\
\beta_1^{(11,2L)S}(\mathrm{q}) &= -\mathrm{q}^L \left[\sqrt{\tfrac{L+1}{L}}\tfrac{\tilde{q}_0}{\mathrm{q}} P^{(11,0L)S}(\mathrm{q}) + \mathrm{q}\sqrt{\tfrac{2L+1}{L}}\hat{P}^{(11,L)S}(\mathrm{q})\right] \\
\beta_1^{(21,\rho L)S}(\mathrm{q}) &= -\mathrm{q}^L\sqrt{2}P^{(01,\rho L)S}(\mathrm{q}) \qquad (\rho=0,1) \\
\beta_1^{(21,2L)S}(\mathrm{q}) &= \mathrm{q}^L\sqrt{2}\left[\sqrt{\tfrac{L+1}{L}}\tfrac{\tilde{q}_0}{\mathrm{q}} P^{(01,0L)S}(\mathrm{q}) + \mathrm{q}\sqrt{\tfrac{2L+1}{L}}\hat{P}^{(01,L)S}(\mathrm{q})\right]
\end{aligned}
\tag{31}
$$

As an example, equations (32) and (33) give the “generalized polarizabilities” in two important cases :

$$
\begin{aligned}
P^{(01,01)0}(\mathrm{q}) = \sqrt{\frac{2}{3}}\ \ & \textstyle\sum_{(X\neq N)} [< N|d(0)|X >< X|d(\mathrm{q})|N > \\
& + < N|d(\mathrm{q})|X >< X|d(0)|N >]\, \frac{1}{m-m_X}
\end{aligned}
\tag{32}
$$

$$
d(\mathrm{q}) = \int d\vec{r}\frac{3j_1(\mathrm{q}r)}{\mathrm{q}r}J^0(\vec{r})z
$$

$$
\begin{aligned}
P^{(11,11)0}(\mathrm{q}) = \frac{4}{\sqrt{6}}\ \ & \textstyle\sum_{(X\neq N)} [< N|\mu(0)|X >< X|\mu(\mathrm{q})|N > \\
& + < N|\mu(\mathrm{q})|X >< X|\mu(0)|N >]\, \frac{1}{m-m_X}
\end{aligned}
\tag{33}
$$

$$
\mu(\mathrm{q}) = \frac{1}{2}\int d\vec{r}\frac{3j_1(\mathrm{q}r)}{\mathrm{q}r}\left[\vec{r}\times\vec{J}\right]_z
$$

where J^μ is the hadronic current. When $\mathrm{q}\to 0$, $[3j_1(\mathrm{q}r)/\mathrm{q}r]\to 1$ so that, up to a constant factor, we recognize in equations (32, 33) the usual electric (α) and magnetic (β) polarizabilities of the nucleon. Explicitly :

$$
P^{(01,01)0}(0) = -\sqrt{\frac{2}{3}}\frac{\bar{\alpha}}{e^2}, \qquad P^{(11,11)0}(0) = -\sqrt{\frac{8}{3}}\frac{\bar{\beta}}{e^2}
\tag{34}
$$

where $\bar{\alpha}$ and $\bar{\beta}$ are in the Gaussian units, e^2=1/137.
It should be clear that the measurement of these “generalized polarizabilities” through Virtual Compton Scattering will enlarge enormously the set of electromagnetic observables against which the nucleon structure models can be compared.

According equations (24,25,28) and the low energy theorem due to Low, the experiment near threshold ($\mathrm{q}'\le m_\pi$) has to determine $\mathcal{M}^{exp}$ in the form :

$$
\mathcal{M}^{exp} = \frac{\mathcal{M}^{exp}_{-2}}{\mathrm{q}'^2} + \frac{\mathcal{M}^{exp}_{-1}}{\mathrm{q}'} + \mathcal{M}^{exp}_0 + 0(\mathrm{q}')
\tag{35}
$$

where the coefficients $\mathcal{M}^{exp}_i$, i=-2,-1,0 are functions of $(\mathrm{q},\epsilon,\theta,\varphi)$.
One defines (see Ref. [7]) :

$$
\frac{1}{4}\sum_{\sigma\sigma' h'\lambda'}|T^{BH}+T^{Born}|^2 = \frac{\mathcal{M}^{LET}_{-2}}{\mathrm{q}'^2} + \frac{\mathcal{M}^{LET}_{-1}}{\mathrm{q}'} + \mathcal{M}^{LET}_0 + 0(\mathrm{q}')
\tag{36}
$$

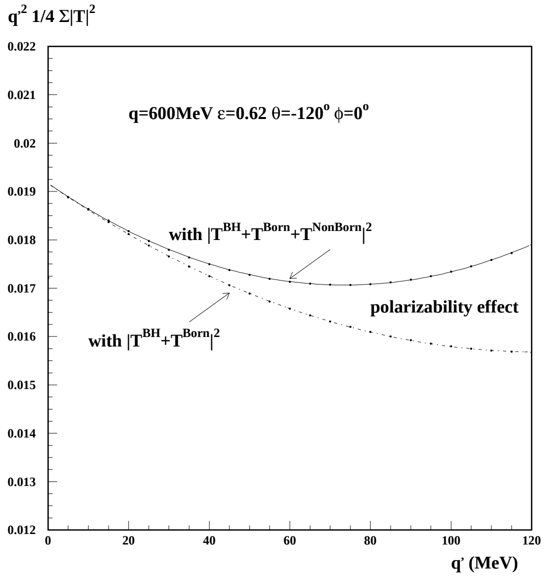

Figure 3: *The experimental method consits to study the evolution of $q'^2 \times \mathcal{M}^{exp}$ at fixed $(q, \epsilon, \theta, \varphi)$. In a polynomial fit, the parameter of the second order in q' will provide the LET prediction plus the polarizability effect.*

The coefficients $\mathcal{M}_i^{LET}$, i=-2,-1,0 are calculable functions of $(\mathrm{q}, \epsilon, \theta, \varphi)$.

The experimental method (see Fig. 3) is to study the evolution of $\mathrm{q}'^2\mathcal{M}^{exp}$ with small values of q′ at fixed values of $(\mathrm{q}, \epsilon, \theta, \varphi)$. In a polynomial fit the two first terms (ordinate and slope at the origin) have to be the same than those which are given by the LET expansion :

$$\mathcal{M}_{-2}^{exp}(\mathrm{q}, \epsilon, \theta, \varphi) = \mathcal{M}_{-2}^{LET}(\mathrm{q}, \epsilon, \theta, \varphi) \tag{37}$$

$$\mathcal{M}_{-1}^{exp}(\mathrm{q}, \epsilon, \theta, \varphi) = \mathcal{M}_{-1}^{LET}(\mathrm{q}, \epsilon, \theta, \varphi) \tag{38}$$

This is a crucial part of the experiment because it validates the expansion assumed in equation (35) and the following step which is the extraction of the "generalized" polarizabilities.

Then the parameter of the second order in q′, $\mathcal{M}_0^{exp}$ will provide $\mathcal{M}_0^{LET}$ plus an extra term, which is a linear combination of the "generalized" polarizabilities. This term is due to the interference between $T^{BH} + T^{Born}$ and $T^{NonBorn}$ (product $\alpha_{-1}\beta_1$ in equation (28)). We can write :

$$\mathcal{M}_0^{exp} - \mathcal{M}_0^{LET} = \sum_{i=1}^{10} c_i(\mathrm{q}, \epsilon, \theta, \varphi).P_i(\mathrm{q}) \tag{39}$$

where $c_i(\mathrm{q}, \epsilon, \theta, \varphi)$ are kinematical coefficients and $P_i(\mathrm{q})$ are the "generalized" polarizabilities.

With an unpolarized experiment, we can extract only 4 linear combinations of the "generalized" polarizabilities. An experiment using polarized beam and focal plane polarimeter for the outgoing proton will give access to more combinations of the polarizabilities. These experiments are planned at MAMI and CEBAF.

In order to extract the "generalized" polarizabilities $P_i(\mathrm{q})$ we have to play with different values of $c_i(\mathrm{q}, \epsilon, \theta, \varphi)$ (that is, to vary $(\epsilon, \theta, \varphi)$ when q is fixed) in order to change the interference between the BH and $FVCS$ terms. The left part of Fig. 4 represents the three contributions

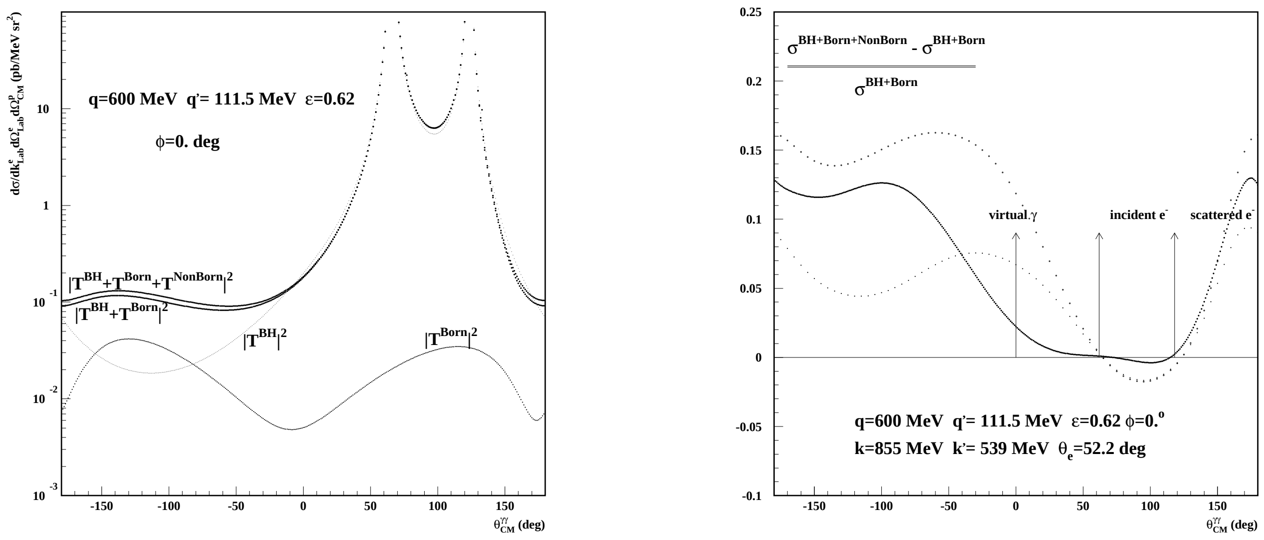

Figure 4: <u>On left</u> : *The contributions* $|T^{BH}|^2$*,* $|T^{Born}|^2$*,* $|T^{BH}+T^{Born}|^2$*,* $|T^{BH}+T^{Born}+T^{NonBorn}|^2$ *are indicated in a logarithmic scale in the kinematical domain studied at MAMI. The "generalized" polarizabilities introduced in the Non Born term are estimated in the NRQCM.* <u>On right</u> *: Effect of the polarizabilities : The deviation* $(\sigma_{BH+Born+\Delta}-\sigma_{BH+Born})/\sigma_{BH+Born}$ *is estimated by 2 models : the NRQCM (in solid line) and an effective lagrangien model which includes different resonances (only* $\Delta(1232)$ *in top-dotted line and all the first dominant resonances as* $\Delta(1232)$*,* P_{11}*(1440),* D_{13}*(1520),* S_{11}*(1535) in bottom-dotted line).*

to the cross sections of respectively $|T^{BH}|^2$, $|T^{Born}|^2$, and $|T^{BH}+T^{Born}|^2$ as a function of $\theta_{lab}^{\gamma\gamma}$ in the domain studied at MAMI (q = 600 MeV, q′ = 67.5 MeV, $\epsilon = 0.62$, $\varphi = 0$). As it is well known the BH process is strongly peaked along the electron lines. This allows us to define regions in (θ, φ) for the final photon where BH is either dominant or comparable to the $FVCS$, thereby favouring the interference. As $\varphi = 0$, the promising region is from $\theta_{CM}^{\gamma\gamma} = -180°$ to $0°$.

Two estimates of the generalized polarizabities have been already determined.

- One is realized in the Non Relativistic Constituent Quark Model [7]. The corresponding effect is reported in Fig. 4 in the term $|T^{BH}+T^{Born}+T^{NonBorn}|^2$. The deviation relative to the LET,viz. $(\sigma_{BH+Born+\Delta}-\sigma_{BH+Born})/\sigma_{BH+Born}$, is shown more clearly in the right part of Fig. 4 by the solid line.

- Another calculation has been realized with an effective Lagrangian [13] which includes only the $\Delta(1232)$ resonance (top-dotted line in Fig. 4) or all the dominant resonances as $\Delta(1232)$, $P_{11}(1440)$, $D_{13}(1520)$, $S_{11}(1535)$ (bottom-dotted line).

All these estimations give an order of magnitude of the deviation of 10%, so only a very precise study of the Virtual Compton Scattering will allow the measurement of "generalized" polarizabilities.

Due to the Lorentz boost from the Centre of Mass to the Laboratory frames, the outgoing proton momentum tends to be focused in a small cone around the virtual photon momentum.

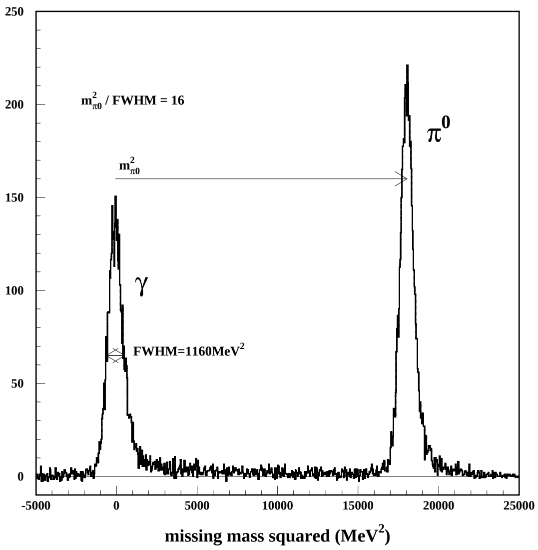

Figure 5: *The experimental spectrum of the missing mass (in MeV^2) in the reaction $p(e,e'p)X$ with a very good separation between Compton and π^0 electroproduction events.*

Thus a large phase space for the real photon is accessible in a single measurement of a coincidence between the scattered electron and the recoil proton detected in two spectrometers, despite the small solid angles.

With the high duty cycle available at MAMI, we are not limited by the accidental counting rates, and we can use the maximum luminosity. A typical luminosity of $\mathcal{L} = 2.10^{37}$ cm^{-2} s^{-1} which corresponds to a 40 μA beam current on a 2 cm length liquid hydrogen target, was used during the first test in March 1995 at MAMI.

We measure seven experimental observables, the incident beam energy, the momenta and angles of the scattered electron and of the recoil proton : $(\mathrm{k}_{lab}, \mathrm{k}'_{lab}, \mathrm{p}'_{lab}, \theta_{e_{lab}}, \theta_{p_{lab}}, \varphi_{e_{lab}}, \varphi_{p_{lab}})$ With these quantities, we reconstruct the missing mass m_X^2 (see Fig. 5). The $e+p \rightarrow e'+p'+\gamma$ events are characterized by the photon mass: $m_X^2 = 0$, which is clearly separated from the π^0 contribution at $m_X^2 = 0.0182$ GeV^2 thanks to the excellent resolution given by the facilities at MAMI (very good resolutions for beam $\Delta\mathrm{k}_{lab}/\mathrm{k}_{lab} = 10^{-4}$ and spectrometers $\Delta\mathrm{k}'_{lab}/\mathrm{k}'_{lab} = \Delta\mathrm{p}'_{lab}/\mathrm{p}'_{lab} = 10^{-4}$, angular resolution better than 3 mrad)

3 Gerasimov-Drell-Hearn sum rule verification

The Gerasimov-Drell-Hearn (GDH) [14] sum rule relates the helicity structure of the total cross section of polarized photons on polarized nucleons to the anomalous magnetic moment of the nucleon. It is based on Lorentz and gauge invariance, crossing symmetry, causality and unitarity. The precise value of this sum rule will provide some constraints on the nucleon models. This prediction was formulated in the 1960's, but has never been tested experimentally because the technical developments on the polarized beam were not yet available.

The GDH sum rule is nowadays of particular interest as it is connected to sum rules on the g_1 polarized structure function of the nucleon at high momentum transfer. Many recent experiments have been realized in deep inelastic scattering in order to probe the parton spin distribution. Because non-perturbative QCD corrections might influence the interpretation of these measurements, considerable attention have recently be paid to the Q^2 evolution of the spin observables.

Many experiments are already forseen to verify the $Q^2 = 0$ limit (GDH sum rule) and its evolution at low Q^2 (at MAMI and ELSA, LEGS and GRAAL, CEBAF).

3.1 Derivation of the GDH sum rule and other sum rules

The Gerasimov-Drell-Hearn (GDH) sum rule deals with the absorption of circularly polarized photons by longitudinally polarized nucleons. The two relative spin configurations - parallel or antiparallel - correspond to the two absorption cross sections $\sigma_{3/2}$ and $\sigma_{1/2}$. This sum rule predicts that the integral over the energy ν of the difference of these two cross sections, weighted by the inverse of the energy, is related to static properties of the nucleon, the mass m and the anomalous magnetic momentum κ in the following way :

$$\int_0^\infty d\nu \frac{\sigma_{1/2} - \sigma_{3/2}}{\nu} = -\frac{2\pi^2 \alpha_{QED}}{m^2} \kappa^2 \tag{40}$$

The GDH sum rule is derived from very general principles applied on the Compton forward amplitude on the nucleon (with polarization measurement and $\theta = 0$ by comparison with the formula (20)). The general ansatz for this amplitude can be written out between initial and final nucleon Pauli spinors χ_i and χ_f and initial and final real photon polarization vectors $\vec{\epsilon}$ and $\vec{\epsilon'}$ (the initial and final photon energy is ν) :

$$f(\nu) = \chi_f^* (f_1(\nu) \vec{\epsilon'^*} . \vec{\epsilon} + i f_2(\nu) \vec{\sigma} . (\vec{\epsilon'^*} \times \vec{\epsilon})) \chi_i \tag{41}$$

If we average over nucleon spins we are left with f_1 which is the spin averaged forward amplitude. To obtain f_2 we need polarization. If we use circularly polarized photons, the amplitudes for parallel and antiparallel relative spin configurations of the nucleon and the photon, yield respectively the difference and the sum of f_1 and f_2.

$$f_{3/2} = f_1 - f_2 \text{ and } f_{1/2} = f_1 + f_2 \quad \text{or} \quad f_1 = (f_{3/2} + f_{1/2})/2 \text{ and } f_2 = (f_{3/2} - f_{1/2})/2 \tag{42}$$

From crossing symmetry, we can deduce that f_1 is an even, and f_2 an odd function of ν :

$$f_1(\nu) = f_1^*(-\nu) \qquad \text{and} \qquad f_2(\nu) = -f_2^*(-\nu) \tag{43}$$

The sum rule is derived using the very general principles of causality, unitarity, relativity and gauge invariance. The only questionable assumption is the no-subtraction hypothesis in writing the dispersion relation for the forward Compton amplitude. We therefore consider this question in some detail. Causality implies analitycity of the amplitude in the complex plane :

$$f(\nu) = \lim_{\epsilon \to 0} f(\nu + i\epsilon) \tag{44}$$

The Cauchy relation allows one to write :

$$f(z) = \frac{1}{2i\pi}\int_{\mathcal{C}} \frac{f(\nu')}{\nu' - z}d\nu' \overset{if...}{\rightarrow} \frac{1}{2i\pi}\int_{-\infty}^{+\infty} \frac{f(\nu')}{\nu' - z}d\nu' \tag{45}$$

where $\mathcal{C}$ is a contour included z where the function is analytically continue. $\mathcal{C}$ can be described by the real axis from $-\infty$ to $+\infty$, added by an half-circle of radius R which goes to ∞.
If $f(\nu')$ goes to 0 when ν' goes to ∞ more rapidly than $1/\nu'$, then the contribution on the half-circle vanishes, and we are left with only the integral on the real axis. The Cauchy relation gives :

$$\lim_{\epsilon\to 0} \frac{1}{x \pm i\epsilon} = \mathcal{P}(\frac{1}{x}) \mp i\pi\delta(x) \tag{46}$$

where the principal part is noted $\mathcal{P}$. Then with these three last relations, we can write :

$$f(\nu) = \lim_{\epsilon\to 0}\frac{1}{2i\pi}\int_{-\infty}^{+\infty}\frac{f(\nu')}{\nu' - \nu - i\epsilon}d\nu' = \frac{1}{2i\pi}\mathcal{P}\int_{-\infty}^{+\infty}\frac{f(\nu')}{\nu' - \nu}d\nu' + \frac{1}{2}f(\nu) \tag{47}$$

If we take only the real part of the 2 members, we obtain a dispersion relation (by analogy with optics) between the real and imaginary part of $f(\nu)$:

$$\Re e f(\nu) = \frac{1}{\pi}\mathcal{P}\int_{-\infty}^{+\infty}\frac{\Im m f(\nu')}{\nu' - \nu}d\nu' \tag{48}$$

The convergence assumption can be improved by making "subtractions". Effectively the assumption $\frac{f(\nu')}{\nu' - \nu_0} \overset{\nu'\to\infty}{\rightarrow} 0$ is easier realized than $f(\nu') \overset{\nu'\to\infty}{\rightarrow} 0$ (ν_0 is a pole of the new considered function). The Cauchy relation is then :

$$\frac{f(z)}{z - \nu_0} - \frac{f(\nu_0)}{z - \nu_0} = \frac{1}{2i\pi}\int_{\mathcal{C}}\frac{f(\nu')}{(\nu' - \nu_0)(\nu' - z)}d\nu' \tag{49}$$

The corresponding dispersion relation has now a "subtracted" term :

$$\Re e f(\nu) = \Re e f(\nu_0) + \frac{\nu - \nu_0}{\pi}\mathcal{P}\int_{-\infty}^{+\infty}\frac{\Im m f(\nu')}{(\nu' - \nu_0)(\nu' - \nu)}d\nu' \tag{50}$$

Now we can derive the sum rule using the three following fundamental principles :

1. Causality implies analyticity which allows writing the forward amplitude dispersion relation without subtraction and simplifying according crossing symmetry :

$$\Re e f_1(\nu) = \frac{1}{\pi}\mathcal{P}\int_{-\infty}^{\infty} d\nu' \frac{\Im m\, f_1(\nu')}{\nu' - \nu} = \frac{2}{\pi}\mathcal{P}\int_0^{\infty} d\nu'\nu'\frac{\Im m\, f_1(\nu')}{\nu'^2 - \nu^2} \tag{51}$$

$$\Re e f_2(\nu) = \frac{1}{\pi}\mathcal{P}\int_{-\infty}^{\infty} d\nu' \frac{\Im m\, f_2(\nu')}{\nu' - \nu} = \frac{2\nu}{\pi}\mathcal{P}\int_0^{\infty} d\nu'\frac{\Im m\, f_2(\nu')}{\nu'^2 - \nu^2} \tag{52}$$

It is easy to verify that the crossing symmetry implies a better convergence to the f_2 integral than for the f_1 integral.

2. Flux conservation implies unitarity which is expressed in the optical theorem :

$$\Im m f_1(\nu) = \frac{\nu}{8\pi}(\sigma_{1/2} + \sigma_{3/2}) = \frac{\nu}{4\pi}\sigma_{tot} \qquad \text{and} \qquad \Im m f_2(\nu) = \frac{\nu}{8\pi}(\sigma_{1/2} - \sigma_{3/2}) \tag{53}$$

3. For small values of the photon energy ν, the functions f_1 and f_2 can be written as :

$$f_1(\nu) = -\frac{\alpha_{QED}}{m} + (\bar{\alpha} + \bar{\beta})\nu^2 + 0(\nu^4) \tag{54}$$

$$f_2(\nu) = -\frac{\alpha_{QED}\kappa^2}{2m^2}\nu + \gamma\nu^3 + 0(\nu^5) \tag{55}$$

The leading term in the spin-independent amplitude describes Thomson scattering which depends on mass and charge and is a simple consequence of gauge invariance. The corresponding spin-dependent term is given by the low energy theorem of Low, Gell-Mann and Goldberger[15] and appears as a consequence of both gauge and relativistic invariance. The second terms correspond respectively to the electric and magnetic polarizabilities $(\bar{\alpha} + \bar{\beta})$ of the nucleon (as we have seen in a previous section), and the spin polarizability (γ) (defined by analogy).

By combining the 2 first points and doing an expansion in power of ν we obtain :

$$f_1(\nu) = \frac{1}{2\pi^2}\int_0^\infty \sigma_{tot}(1 + \frac{\nu^2}{\nu'^2} + ...)d\nu' \tag{56}$$

$$f_2(\nu) = \frac{1}{4\pi^2}\int_0^\infty (\sigma_{1/2} - \sigma_{3/2})(\frac{\nu}{\nu'} + \frac{\nu^3}{\nu'^3} + ...)d\nu' \tag{57}$$

If we compare the expansion of f_2 with the third item we obtain both :

- the GDH sum rule :

$$\left(\frac{\partial}{\partial\nu}\right)[f_2(\nu)]_{\nu=0} = \frac{1}{4\pi^2}\int_0^\infty d\nu'\frac{\sigma_{1/2} - \sigma_{3/2}}{\nu'} = -\frac{\alpha_{QED}\kappa^2}{2m^2} \tag{58}$$

- the γ polarizability sum rule :

$$\left(\frac{\partial}{\partial\nu}\right)^3[f_2(\nu)]_{\nu=0} = \frac{1}{4\pi^2}\int_0^\infty d\nu'\frac{\sigma_{1/2} - \sigma_{3/2}}{\nu'^3} = \gamma \tag{59}$$

Nevertheless, the expansion of f_1 will give an absurd expression :

$$f_1(0) = \frac{1}{2\pi^2}\int_0^\infty d\nu'\sigma_{tot} = -\frac{\alpha_{QED}}{m}! \tag{60}$$

The convergence of f_1 is made worse because of the crossing symmetry law and therefore we need at least one subtraction :

$$\Re e f_1(\nu) - f_1(0) = \frac{\nu}{\pi}\mathcal{P}\int_{-\infty}^\infty d\nu'\frac{\Im m\, f_1(\nu')}{\nu'(\nu' - \nu)} = \frac{2\nu^2}{\pi}\mathcal{P}\int_0^\infty d\nu'\frac{\Im m\, f_1(\nu')}{\nu'(\nu'^2 - \nu^2)} \tag{61}$$

Then :

$$f_1(\nu) = -\frac{\alpha_{QED}}{m} + \frac{1}{2\pi^2}\int_0^\infty \sigma_{tot}(\frac{\nu^2}{\nu'^2} + \frac{\nu^4}{\nu'^4} + ...)d\nu' \tag{62}$$

And we obtain the electric and magnetic polarizabity sum rule :

$$\left(\frac{\partial}{\partial\nu}\right)^2[f_2(\nu)]_{\nu=0} = \frac{1}{2\pi^2}\int_0^\infty d\nu'\frac{\sigma_{tot}}{\nu'^2} = \bar{\alpha} + \bar{\beta} \simeq (14.2 \pm 0.3)10^{-4} fm^3 \tag{63}$$

The necessity for subtraction in the f_1 dispersion relation can also be demonstrated in the Regge poles model where the scattering amplitude at high energy is expressed as a sum of terms :

$$\Im m f(\nu) = \sum_i c_i \nu^{\alpha - i} \tag{64}$$

each corresponding to the exchange in the t channel of a given Regge pole. We need to know the intercept at t=0 of the corresponding Regge trajectory, $\alpha_i(0)$, which can be considered as the apparent value of the angular momentum of the exchanged object at zero momentum transfer. The asymptotic behaviour is determined by the highest $\alpha(0)$ value. The relevant trajectories in the case of f_1 are the Pomeron, the P' and the A_2, which intercepts are respectively 1, 1/2, 1/2. The asymptotic behaviour of f_1 is :

$$\Im m f_1(\nu) = c_1 \nu + c_2 \sqrt{\nu} \tag{65}$$

and the integrand of the non subtracted relation dispersion is a constant for large energies. Therefore the dispersion integral does not converge : we need to realize one subtraction which insures a better convergence.

In the case of f_2 the corresponding Regge trajectories are not so well known. Nevertheless, the spin dependence of the cross sections has to become insignificant at very high energies in order to provide a good convergence. The sign of the GDH sum rule gives a larger contribution of $\sigma_{3/2}$ than of $\sigma_{1/2}$, but due to the large contribution of the $\Delta(1232)$ resonance (at Q^2=0), it is quite possible !

3.2 Connections with Deep Inelastic Scattering

The GDH sum-rule is connected with the sum-rules on the g_1 polarized structure function of the nucleon. In the more general case of circularly polarized virtual transverse photons - squared mass $-Q^2$, energy ν -, the difference of the two elementary absorption cross sections $\sigma_{1/2}$ and $\sigma_{3/2}$ can be expressed in term of two polarized structure functions $G_1(\nu, Q^2)$ and $G_2(\nu, Q^2)$.

$$\sigma_{1/2} - \sigma_{3/2} = \frac{8\pi^2 \alpha}{\nu - Q^2/2m} (m\,\nu\, G_1(\nu, Q^2) - Q^2 G_2(\nu, Q^2)) \tag{66}$$

In both cases of deep inelastic scattering and real photon absorption the contribution of the second term vanishes and $\sigma_{1/2} - \sigma_{3/2}$ is expressed simply in terms of G_1.

Anselmino et al.[16] have considered the quantity of interest $I(Q^2)$.

$$I(Q^2) = m^3 \int_{Q^2/2m}^{\infty} d\nu \frac{G_1(\nu, Q^2)}{\nu} = \frac{2m^2}{Q^2} \int_0^1 dx\ g_1(x, Q^2) \tag{67}$$

where $x = Q^2/2m\nu$ is the relevant kinematical quantity.

Several experiments EMC [17], SMC [18], E142 [19], E143 [20] were devoted to measuring $\int_0^1 dx\ g_1(x, Q^2)$ at different Q^2 (respectively 10.7, 4.6, 2., 3. GeV^2). EMC and E143 provide a direct measurement of the value for the proton, while SMC and E142 give the value for the neutron via deuterium and He^3 nuclei targets respectively.

For the proton, EMC and E143 have provided really compatible values of $\int_0^1 dx\ g_1(x,Q^2)$:

$$\begin{array}{llll} \int_0^1 dx\ g_1^p(x,Q^2) = 0.128 \pm 0.013 \pm 0.019 & Q^2 = 10.7\mathrm{GeV}^2 & \mathrm{EMC} \\ \int_0^1 dx\ g_1^p(x,Q^2) = 0.127 \pm 0.004 \pm 0.010 & Q^2 = 3.0\mathrm{GeV}^2 & \mathrm{E143} \end{array} \quad (68)$$

In the quark parton model the structure function $g_1(x)$ is related to the difference of the quark distributions for quarks with helicity parallel and antiparallel to the nucleon spin. Using the properties of current algebra we obtain with this experimental value that the total spin carried by all the quarks and antiquarks in the proton is only of the order of 20%.

For the isovector combination proton-neutron, there is the very fundamental Bjorken sum-rule [22] at large Q^2 based on quark current algebra, which relates the difference of the two integrals on proton and on neutron to the neutron beta decay coupling constants, with QCD corrections :

$$\int_0^1 dx(g_1^p(x,Q^2) - g_1^n(x,Q^2)) = \frac{1}{6}\frac{g_A}{g_V}(1 - \frac{\alpha_s(Q^2)}{\pi}) \quad (69)$$

With all the experimental data, Ellis and Karliner have extracted $\int_0^1 dx(g_1^p(x,Q^2) - g_1^n(x,Q^2))$ at $Q^2 = 2.0$ GeV^2 and 4.6 GeV^2, which are compatible with the Bjorken sum rule within one standard deviation.

$$\begin{array}{llll} \int_0^1 dx\ (g_1^p(x,Q^2) - g_1^n(x,Q^2)) = 0.152 \pm 0.014 \pm 0.021 & Q^2 = 2.0\mathrm{GeV}^2 & \mathrm{E142/EMC} \\ \int_0^1 dx\ (g_1^p(x,Q^2) - g_1^n(x,Q^2)) = 0.201 \pm 0.048 \pm 0.042 & Q^2 = 4.6\mathrm{GeV}^2 & \mathrm{SMC/EMC} \end{array} \quad (70)$$

On the other hand for real photons, the GDH sum-rule predicts :

$$I(0) = \frac{m^2}{8\pi^2\alpha}\int_0^\infty d\nu\ \frac{\sigma_{1/2} - \sigma_{3/2}}{\nu} = -\frac{\kappa^2}{4} \quad (71)$$

$$I^p(0) = -0.804 \quad \text{and} \quad I^{p-n}(0) = +0.112 \quad (72)$$

Fig. 6 summarizes the different experimental and theoretical determinations of $I(Q^2)$ for the proton and the isovector combination proton-neutron. In the case of the proton we observe a change of sign from the deep inelastic regime as measured by EMC to the real photon point predicted by the GDH sum-rule. For the proton-neutron combination, the Bjorken sum-rule prediction seems to extrapolate rather smoothly to the GDH value. The higher twist contributions with the non-perturbative effects, which are supposed to explain the proton behaviour at low Q^2, seem to cancel out in the p-n case. An experimental check of the GDH sum-rule (at Q^2=0) could ascertain this intriguing situation. This will be done at MAMI and ELSA, and LEGS and GRAAL. Some other experiments in order to study the evolution as the sum rule at low Q^2 (≤ 1.5 GeV^2) will be performed at CEBAF.

3.3 Estimates from Photoproduction Multipoles

In absence of direct observation of the helicity-dependent cross sections, it is possible to make an estimate of the GDH sum rule integrals using existing multipole analyses constructed from mesurements of the different charge channels in meson production. To do this, an

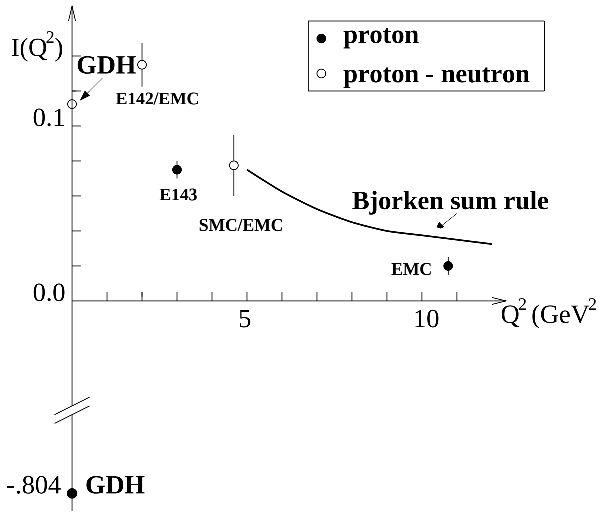

Figure 6: *The quantity $I(Q^2)$ defined by Anselmino. The experimental value given by the EMC, SMC, E142 and E143, and the predictions provided by the Bjorken sum-rule and the Drell-Hearn-Gerasimov sum-rule are presented.*

isospin decomposition of the integrals is made, producing three components : the isovector(vv), isoscalar (ss) and mixed (vs) terms. This decomposition gives :

$$\begin{aligned} \int_0^\infty d\nu \frac{\sigma^{vv}_{1/2}-\sigma^{vv}_{3/2}}{\nu} &= -\frac{2\pi^2\alpha_{QED}}{m^2}\kappa_v^2 \\ \int_0^\infty d\nu \frac{\sigma^{vs}_{1/2}-\sigma^{vs}_{3/2}}{\nu} &= -\frac{2\pi^2\alpha_{QED}}{m^2}\kappa_v\kappa_s \\ \int_0^\infty d\nu \frac{\sigma^{ss}_{1/2}-\sigma^{ss}_{3/2}}{\nu} &= -\frac{2\pi^2\alpha_{QED}}{m^2}\kappa_s^2 \end{aligned} \tag{73}$$

The fact that the integrals are weighted towards small energies hints that the resonance region may be relevant in the sum rule. A sizeable contribution to the sum-rule comes from single pion photoproduction. Using the multipole analysis of the data, I. Karliner [23] in 1973 and more recently Workman and Arndt [28] in 1992 (which include new sets of high precision data) have computed the single pion contribution to the GDH sum-rule for the proton and the neutron, see table 2. The result is complemented by some estimate of the inelastic contributions done by I. Karliner. The large isovector (vv) component obtained in these multipole analyses appears to be stable and in quite reasonable agreement with the sum rule value. Similarly, the total isoscalar (ss) contribution remains consistently small, as is the corresponding GDH value. Nevertheless, there is a large and significant discrepancy in the vector-scalar (vs) contribution in magnitude and sign. The better knowledge of the multipoles has made the situation worse. Further refinements will require double-polarization data which will be provided at the same time as the investigation of the sum rule. We have also to point that the sum rule is a very delicate cancellation of individual multipoles [26]. So a very systematic study on both proton and neutron is necessary before any early conclusion.

It seems necessary to study the spin-dependent effects in the resonance region to probe the non-perturbative dynamics [24] and to measure precisely the difference between the two

	$\int_0^{1.2GeV} d\nu\ \frac{\sigma_{1/2}-\sigma_{3/2}}{\nu}$ multipole analysis			$\int_0^{1.7GeV} d\nu\ \frac{\sigma_{1/2}-\sigma_{3/2}}{\nu}$ multipole analysis			$\int_0^{\infty} d\nu \frac{\sigma_{1/2}-\sigma_{3/2}}{\nu}$ GDH
	Karliner Nπ	Karliner N$\pi\pi$	Total	Workman-Arndt Nπ	Karliner N$\pi\pi$	Total	
vv	-170	-49	-219	-178	-49	-227	-218.5
ss	-2	-1	-3	+3	-1	+2	-0.3
vs	-24	-15	-39	-50	-15	-65	+14.7
proton			-261			-289	-204.1
neutron			-183			-160	-233.5

Table 2: The isospin decomposition (in μb) of the GDH integral calculated from pion photoproduction multipole analysis and compared to the GDH predictions.

polarized absorption cross section $\sigma_{3/2}$ and $\sigma_{1/2}$ on the proton and the neutron in an energy domain from pion threshold, to at least 3 GeV. This will be realized at MAMI and ELSA. The experiment will start next year.

4 Outlook on exclusive and hard reactions

Exclusive and hard reaction studies will be one of the greater topic investigated at ELFE. Exclusive electroproduction processes are needed to study the spatial structure of hadrons, such as form factors of mesons or transition form factors for baryon resonances (completely analogous to elastic form factors). Because exclusive processes require coherent scattering off quarks the results are sensitive to the hadron wave function in terms of quarks.

In order to have an intuitive interpretation of an exclusive and hard process, eg. $\gamma p \to p'\gamma'$, at large s and large t (even $Q^2 = 0$) we must imagine that an elementary parton in the target nucleon is struck by the incoming photon. To build the defined final particles emitted at large angle from the incident direction, this first active parton has to inform at least $n-1$ partons ($n = 3$ is the valence number for the final proton), which are at some small distances of the order $1/s$ or $1/t$. All configuration which will involve extra partons will have a smaller probability. Thus, we have a way to select preferentially the valence quark contributions. Moreover, since only small distances between the acting participants are investigated, we can use perturbative QCD to calculate the corresponding amplitude. The process can be thought of as proceeding in three stages [1] (see Fig. 7) :

- a soft process (npQCD) where the incident proton is projected in 3 valence quarks
- a hard process described by QCD, where the interaction plays between the acting valence quarks

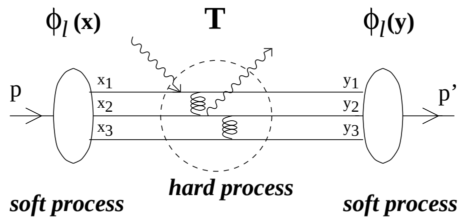

Figure 7: *Factorisation of the hard scattering amplitude*

- a soft process (npQCD) where the 3 valence outgoing quarks are combined to build up the outgoing proton

This is the factorization hypothesis where the exclusive amplitude can be written as :

$$\mathcal{M} =< p|T|p' >= \phi^*(y_j, Q^2) \otimes T(x_i, y_j, Q^2) \otimes \phi(x_i, Q^2) \tag{74}$$

ϕ is the distribution amplitude of 3 valence quarks of momentum fraction x_i and y_j ($i, j = 1, 2, 3$) and T^H is the hard scattering amplitude calculable in the pQCD formalism which has to obey to different fondamental laws :

- hadron helicity conservation (or no transverse polarization quantities at high momentum transfers)
- scaling laws :
  - at high s and t,
  $$\frac{d\sigma}{dt} \sim \frac{1}{s^{n-2}} f(t/s) \tag{75}$$
  where n is the total number of elementary lepton, photon or quark fields entering or leaving the hard scattering subprocess. (In Compton scattering, $n = 8$ for three quarks and one photon present in the initial and final states.)
  - at high Q^2 for the elastic case,
  $$F(Q^2) = (\frac{1}{Q^2})^{n-1} \tag{76}$$
  where n is the number of partons in the hadron

The goal of an exclusive and hard reaction will be to extract the distribution amplitude of valence quarks.

Real Compton scattering has been studied at energies up to $s = 13$ GeV^2 and $t = -4$ GeV^2 [27]. The angular distributions are shown in Fig. 8. An optimistic observer might guess a convergence with the s^{-6} scaling law expected from the dimensional rule (at least viewed on a logarithmic scale). Kronfeld and Nižič have calculated the cross section with four different proton valence quark wave functions which are available at the present time. At finite Q^2, these functions can be written as an expansion in terms of Appel polynomials :

$$\phi(x_1, x_2, x_3, Q^2) = 120 x_1 x_2 x_3 \sum_n a_n(Q^2) A_n(x_1, x_2, x_3) \tag{77}$$

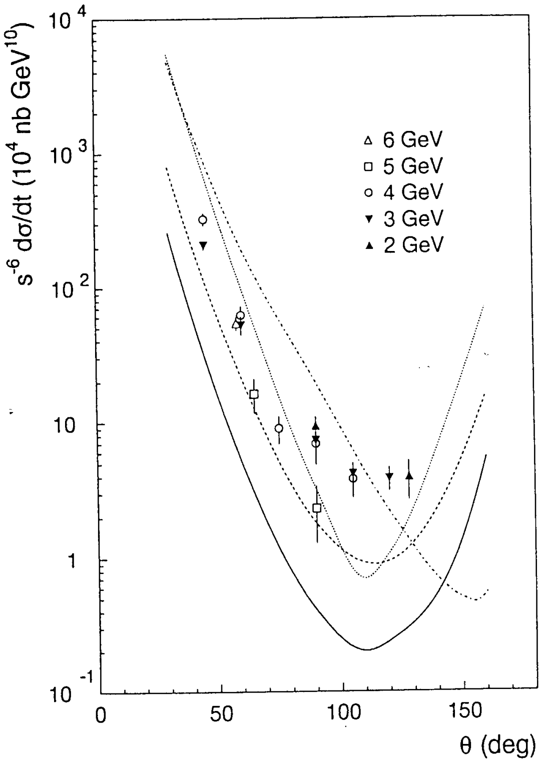

Figure 8: *Compton scattering differential cross section $s^6 d\sigma/dt$. The theoretical curves are obtained using 4 valence quark distribution amplitudes (see Kronfeld and Nižič calculations).*

where A_n are the Appel polynomials and a_n the unknown coefficients governed by confinement dynamics. At present, the expansion of ϕ is truncated after the 6-th term. The difference between these four calculations is really larger than the accuracy of the data. The strategy for the future will be to use this good sensibility and to fit the unknow coefficients of the wave function directly on the data. More precise real Compton scattering data at higher energies would ensure that the asymptotic region is indeed reached and they would shed light on the baryonic structure at high momentum transfer.

References

[1] B. Pire and Th. Gousset, lecture to this ELFE summer school and workshop

[2] G. Anton and B. Krusche, Few-Body Systems Suppl. 99 (1995)
B. Krusche, Phys. Rev. Lett. **74** (1995) 3736

[3] P.E. Bosted et al., Phys. Rev. Lett. **68** (1992) 3841 and L. Andivahis et al., preprint SLAC-PUB-6462 (1994)

[4] R.G. Arnold et al., Phys. rev. Lett. **57** (1986) 174

[5] J. Annand, lecture to this ELFE summer school and workshop
M. Meyerhoff et al., Phys. Lett. **B327** (1994) 201

[6] D. von Harrach et al., proposal at MAMI (1994)

[7] P.A.M. Guichon, G. Liu, A.W. Thomas, Nucl. Phys. **A591** (1995) 606

[8] W. Weise, Baryon Spectroscopy and the Structure of the Nucleon, International Workshop at Saclay, France, 23-25 September, H.P. Morsch and M. Soyeur eds,(1991) 1

[9] B. König, D. Drechsel, L. Tiator, Perspectives on Photon Interactions with Hadrons and Nuclei, Lecture Notes in Physics, Vol. 365 M. schumacher and G. Tamas Eds, (1990) 178

[10] J. Ahrens et al., proposal at MAMI (1995) and references therein.

[11] N. Isgur and G. Karl, Phys. Rev. **D18** (1978) 4187, **D19** (1979) 2653

[12] F.E. Low, Phys. Rev. **96** (1954) 1428

[13] M. Vanderhaeghen, contribution to this ELFE summer school in the parallel session on Real Photons conducted by S. Hall and G. Tamas and Phys. Lett. **B368** (1996) 13

[14] S.B. Gerasimov, Yad. Fiz. **2** (1965) 598, Sov. J. Nucl. Phys. **2** (1966) 430
S.D. Drell and A.C. Hearn, Phys. Rev. Lett. **16** (1966) 908

[15] F. Low, Phys. Rev. **96** (1954) 1428
M. Gell-Mann and M.L. Goldberger, Phys. Rev. **D1** (1970) 1319

[16] M. Anselmino et al., Sov. J. Nucl. Phys. **49** (1989) 136

[17] M.J. Ashman et al., Phys. Lett. **B206** (1988) 364, Nucl. Phys. **B328** (1989) 1

[18] B. Adeva et al., Phys. Lett. **B302** (1993) 533

[19] P.L. Anthony et al., PHys. Rev. Lett. **71** (1993) 959

[20] K. Abe et al., Phys. Rev. Lett. **74** (1995) 346

[21] J. Ellis and M. Karliner, Phys. Lett. **B313** (1993) 131

[22] J.D. Bjorken, Phys. Rev. **179** (1969) 1547

[23] I. Karliner, Phys. Rev. **D7** (1973) 2717

[24] F. Close, Nucl. Phys. **A532** (1991) 25c

[25] R.L.Workman and R.A.Arndt, Phys. Rev. **D45** (1992) 1789

[26] D. Drechsel and M.M. Giannini Few-Body Systems **15** (1993) 99

[27] M.A. Shupe et al., Phys. Rev. **D19** (1979) 1921

[28] A.S. Kronfeld and B. Nižič, Phys. Rev. **D44** (1991) 3445